Published in final edited form as:

DNA Repair (Amst). 2017 March ; 51: 31–45. doi:10.1016/j.dnarep.2017.01.004.

Regulation of human Polλ by ATM-mediated phosphorylation during Non-Homologous End Joining

Guillermo Sastre-Moreno[3], **John M. Pryor**[4], **Marta Moreno-Oñate**[1,2], **Andrés M. Herrero-Ruiz**[2], **Felipe Cortés-Ledesma**[2], **Luis Blanco**[3], **Dale A. Ramsden**[4], and **Jose F. Ruiz**[1,2]

[1]Departamento Bioquímica Vegetal y Biología Molecular, Universidad de Sevilla, Sevilla 41092, Spain

[2]Centro Andaluz de Biología Molecular y Medicina Regenerativa (CABIMER) Universidad de Sevilla/CSIC, Sevilla 41092, Spain

[3]Centro de Biología Molecular “Severo Ochoa”, Universidad Autónoma de Madrid/CSIC, Madrid 28049, Spain

[4]Department of Biochemistry and Biophysics and Curriculum in Genetics and Molecular Biology, Lineberger Comprehensive Cancer Center, University of North Carolina, Chapel Hill, NC 27599, USA

Abstract

DNA double strand breaks (DSBs) trigger a variety of cellular signaling processes, collectively termed the DNA-damage response (DDR), that are primarily regulated by protein kinase ataxia-telangiectasia mutated (ATM). Among DDR activated processes, the repair of DSBs by non-homologous end joining (NHEJ) is essential. The proper coordination of NHEJ factors is mainly achieved through phosphorylation by an ATM-related kinase, the DNA-dependent protein kinase catalytic subunit (DNA-PKcs), although the molecular basis for this regulation has yet to be fully elucidated. In this study we identify the major NHEJ DNA polymerase, DNA polymerase lambda (Polλ), as a target for both ATM and DNA-PKcs in human cells. We show that Polλ is efficiently phosphorylated by DNA-PKcs *in vitro* and predominantly by ATM after DSB induction with ionizing radiation (IR) *in vivo.* We identify threonine 204 (T204) as a main target for ATM/DNA-PKcs phosphorylation on human Polλ, and establish that its phosphorylation may facilitate the repair of a subset of IR-induced DSBs and the efficient Polλ-mediated gap-filling during NHEJ. Molecular evidence suggests that Polλ phosphorylation might favor Polλ interaction with the DNA-PK complex at DSBs. Altogether, our work provides the first demonstration of how Polλ is regulated by phosphorylation to connect with the NHEJ core machinery during DSB repair in human cells.

Correspondence to: Jose F. Ruiz.

Conflict of Interest: The authors declare that they have no conflict of interest.

Author Contributions: J.F.R conceived and designed experiments and wrote the manuscript with advice from the rest of authors. G.S.-M. purified the proteins and performed *in vitro* assays. J.P. performed extrachromosomal NHEJ assays. M. M. O. and A.H.R performed *in vivo* repair assays. J.F.R. performed phosphorylation and interaction assays *in vivo*.

1. Introduction

DNA double-strand breaks (DSBs) constitute one of the most harmful types of damage human cells may undergo, since, when improperly repaired, can generate genomic instability that contributes to development of cancer and human syndromes such as ataxia telangiectasia (AT), Nijmegen breakage syndrome or the Lig4 syndrome [1]. DSBs trigger intracellular signaling processes, collectively termed the DNA-damage response (DDR), that includes cell-cycle checkpoint arrest and repair responses [2]. Protein kinase ataxia-telangiectasia mutated (ATM), a member of the Phosphatidylinositol 3-Kinase-related Kinases (PIKKs) family, acts as an apical activator of DDR modifying hundreds of proteins at specific sites [3]. The fastest pathway for the repair of DSBs is non-homologous end joining (NHEJ), a process that trims and subsequently reconnects broken ends, while requiring only minimal or even null complementarity. Despite its status as the principal DSB repair pathway in most cell cycle stages [4], NHEJ possesses the disadvantage of being inherently error-prone. Indeed, its repair activity can lead to chromosomal translocations [5]. Recent evidence suggests that NHEJ is more complex than a simple cut-and-paste process, with the degree of complexity depending directly on the nature of the DNA ends to be joined [6,7]. In this variable scenario, NHEJ shows an exceptional ability to deal with the wide range of DSBs generated *in vivo* thanks to the many protein factors and enzymatic activities involved in the process [8]. In the first step of NHEJ, DSBs are recognized by the Ku70/Ku80 complex, which protects DNA ends from degradation and acts as a scaffold for the recruitment of other required NHEJ factors [9]. DNA-dependent protein kinase catalytic subunit (DNA-PKcs) is the first protein recruited to DSBs by the Ku70/Ku80 heterodimer, through an interaction with the C-terminus of Ku80, to form the DNA-PK complex [10]. Binding to DNA promotes activation of DNA-PKcs kinase activity, which is essential for the precise coordination of NHEJ machinery according to the configuration of DSB ends. Once activated, DNA-PKcs can phosphorylate a number of NHEJ factors, including Ku70, Ku80, Artemis, XRCC4, the XRCC4-like factor (XLF), and DNA ligase IV [reviewed in 11]. Many of these targets have been well described and their phosphorylation by DNA-PKcs is not required for successful NHEJ *in vivo* [12-14]. To date, DNA-PKcs itself is the only unequivocally defined functionally relevant target of its own kinase activity [15-19]. Following completion of its task at the DSB, DNA-PKcs is autophosphorylated leading to a conformational change that frees the DNA ends and allows NHEJ to proceed [18,19]. As DSBs produced *in vivo* usually have a wide variety of DNA ends, including different configurations and chemical modifications [7], they cannot be directly ligated and must be processed prior to the restoration of DNA integrity. This processing often includes nucleolytic resection of the damaged nucleotides, as well as DNA polymerization to replace the resected DNA and to fill the small gaps generated. Specialized DNA gap-filling synthesis associated with NHEJ in mammalian cells is mainly carried out by PolX family DNA polymerases mu (Polμ) and lambda (Polλ). The participation of Polμ and Polλ in NHEJ is facilitated by their recruitment to DSBs through the interaction with DNA-bound NHEJ core factors, which is primarily mediated by their N-terminal BRCT domain [20-22]. Although both polymerases are able to perform gap-filling reactions, they differ significantly in their optimal substrate and, when active on the same substrate, they often generate distinct products [23,24]. Of the two, Polλ is uniquely effective when 3′-termini are double-

stranded and able to completely fill-in gaps larger than 1 nt [24]. This distinguishing capability is due in part to its ability to scrunch the next-to-be copied template nucleotides in such substrates [25]. Although the physiological role of Polλ in repair of DSBs by NHEJ during VDJ recombination has been established [26], little is known about its regulation during the repair process.

In this work, we identify the phosphorylation of human Polλ by the DDR-related kinases ATM and DNA-PKcs as a novel mechanism of NHEJ regulation in human cells. We show that Polλ is efficiently phosphorylated by DNA-PKcs *in vitro* and we identify threonine 204 (T204), located in the linker serine/proline-rich (S/P-rich) domain, as a main target for such modification. Interestingly, T204 phosphorylation after DSB induction with ionizing radiation *in vivo* is predominantly performed by ATM, and may facilitate Polλ-mediated gap-filling DNA synthesis during NHEJ. Our data suggest that T204 phosphorylation might induce conformational changes in Polλ that stimulate its interaction with DNA-bound NHEJ core factors. In support of this finding, we show that the association of Polλ with Ku80 diminishes after DSBs formation *in vivo* when T204 phosphorylation does not occur properly. Overall, our work describes a novel mechanism of Polλ regulation and contributes to the understanding of the molecular basis of the NHEJ repair process in human cells.

2. Materials and Methods

2.1 Cell culture

Human embryonic kidney 293 cells (293T), human osteosarcoma cells (U2OS) and human melanoma cell lines G361 and HT144 (a kind gift from Dr. Y. Shiloh, Sackler School of Medicine, Tel Aviv University, Israel) were cultured in DMEM medium (Sigma) supplemented with 10% fetal bovine serum (Sigma), 2 mM L-glutamine (Sigma) and antibiotics (100 units/ml penicillin, 100 μg/ml streptomycin) at 37°C in a humidified atmosphere containing 5% CO_2. Mouse embryonic fibroblast cells were cultured as previously described [24].

2.2 Plasmids and RNA interference

The cDNA encoding human POLL was amplified with oligonucleotides *sBglII* (5′-ttgatc AGATCTtatggatcccaggggtatcttg-3′) and *asXbaI* (5′-ttgatcTCTAGAtaaccagtcccgctc-3′) and the PCR product was digested with *BglII* and *XbaI* and cloned in the equally digested p3xFLAG-Myc-CMV Expression Vector (Sigma). POLL phospho-blocking mutants were generated by site-directed mutagenesis starting from the wild-type construct and using oligonucleotides T188A-s (5′-gcaccaaacGcccaagcccagcc-3′), T188A-as (5′-ggctgggcttgggCgtttggtgc-3′), T204A-s (5′-ggggaagaaGcccaggttagtgc-3′) and T204A-as (5′-gcactaacctgggCttcttcccc-3′). Silencing of endogenous POLL was performed by using previously validated siRNAs [27] and two consecutive rounds of transfection with RNAiMAX according to manufacturer's protocol (Life Technologies). To obtain human POLL mutant versions (both T204A phospho-blocking and T204E phospho-mimetic mutants) for protein purification, site-directed mutagenesis was performed using the plasmid pET22b-Polλ [28] as a template with the same oligonucleotides T204A-s and T204A-as described above, and oligonucleotides T204E-s (5′-

GATGATGAAGCCAGTGATGGGGAAGAAGAGCAGGTTAGTGCAGCTGATCTGGAA GCC-3′) and T204E-as (5′-GGCTTCCAGATCAGCTGCACTAACCTGCTCTTCTTCCCCATCACTGGCT TCATCATC-3′), respectively. All constructs were verified by DNA sequencing.

2.3 Immunoprecipitation and immunoblotting

For immunoprecipitations, 2.5×10^5 human 293T cells were seeded per well in 6-well dishes, cultured for 24 h and transiently transfected with p3xFLAG-Myc-CMV expression vector containing either wild-type POLL or POLL-T204A phospho-blocking mutant cDNAs using Gene Juice (Novagen) according to manufacturer's protocol. Forty-eight hours later, cells were either mock-irradiated or irradiated with 10 Gy of IR. At the indicated times post-irradiation, asynchronous cultured cells were washed with cold-phosphate buffered saline (PBS) and collected by low speed centrifugation. Cells were lysed in 500 μL lysis buffer (20 mM Tris-HCl pH 7.5, 150 mM NaCl, 10% glycerol, 2 mM EDTA, 1% NP-40, 1 mM phenylmethylsulfonyl sulfate (PMSF), protease and phosphatase inhibitor cocktails (Sigma) and 1 mM DTT) homogenized and incubated on ice for 30 min. Lysates were cleared by centrifugation at 13,000 rpm for 20 min at 4°C and input (whole cell extract) samples saved for subsequent analysis. Remaining supernatants were incubated with FLAG M2 monoclonal antibody (Sigma) overnight at 4°C according to manufacturer's protocol in the presence of 12 U Benzonase (Millipore). Immuno-complexes were then incubated with Protein G-coupled Dynabeads (Life Technologies) for 4 h with end-to-end mixing at 4°C. Beads were washed three times in lysis buffer and bound immuno-complexes were eluted by boiling in Laemmli buffer at 95°C for 5 min. Proteins were resolved by 10% SDS-PAGE, except in the experiment described in Figure 6B, in which they were resolved by using pre-cast 4-20% gradient SDS-PAGE gels (Biorad). Input lysate (10%) was loaded alongside unless otherwise stated. For the immunoprecipitation of ATM from G361/HT144 cells, whole cell extracts were prepared from these cell lines as described above, and they were incubated with a mouse monoclonal anti-ATM antibody (clone MAT3-4G10/8; Sigma). Immuno-complexes were then treated as described above and finally eluted and used in kinases assays.

For western blot analyses protein extracts were prepared as described above. When indicated, specific inhibitors of ATM (KU55933; ATMi, Tocris; 5 μM) and DNA-PK (NU7441; DNA-PKi, Tocris; 5 μM) or control vehicle (DMSO) were added to cell culture media 1 hour before irradiation. Proteins were resolved by 10% SDS-PAGE, except for ATM and DNA-PKcs immunodetection, that were resolved in pre-cast 4-20% gradient SDS-PAGE gels (BioRad). Then they were transferred onto Immobilon-FL PVDF membranes (Millipore) by using a wet-transfer system (Biorad) at 150 mA for 2 h at 4°C. For the Western blot described in Figure 3D (panel showing FLAG-Polλ electrophoretic mobility using anti-FLAG antibody) protein extracts were run on 6% polyacrylamide long (16 cm) gels and electrophoresis was carried out using a SE600 Hoefer electrophoresis system. Immunoblotting was performed according to Odyssey LI-COR Biosciences protocol. Briefly, membranes were blocked in Odyssey Blocking Buffer (LI-COR) and incubated overnight at 4°C with the primary antibodies at indicated dilution in the same blocking buffer supplemented with 0.1% Tween20. Primary antibodies were used at the following

dilution: mouse monoclonal anti-FLAG M2 (Sigma; 1/5,000), mouse anti-tubulin (Sigma; 1/2,000), rabbit anti-Ku80 (Santa Cruz; 1/1,000), rabbit anti-XRCC4 (Santa Cruz; 1/1,000), rabbit anti-DNA-PKcs (Santa Cruz; 1/1,000), rabbit anti-phospho-DNA-PKcs S2056 (Cell Signaling; 1/2,000), rabbit anti-Polλ (Bethyl; 1/1,000), rabbit anti-phospho Polλ-Thr204 (1/500) and rabbit anti-phospho (Ser/Thr) ATM/ATR substrate (Cell Signaling; 1/1,000). After washes with TBS-0.1% Tween20, membranes were incubated with the corresponding secondary antibodies (IRDyes 800CW for rabbit and/or 680RD for mouse primary antibodies, respectively 1/15,000; LI-COR Biosciences) supplemented with 0.1% Tween20. After washes, membranes were allowed to dry and then analyzed in Odyssey imaging system with the ImageStudio Odyssey CLx Software (LI-COR). Quantification of relative band intensities was carried out using ImageJ software.

2.4 Immunofluorescence

To analyze 53BP1 foci repair kinetics, approximately 4×10^4 U2OS cells were seeded onto sterile glass coverslips in each well of a 4-well dish, cultured for 24 h and transfected with the indicated siRNAs as described above. Twenty-four hours later, cells were subjected to a second siRNA transfection as described above and incubated for 48 additional hours. After this time, cells were mock irradiated or irradiated with 10 Gy, and fixed with 4% paraformaldehyde in PBS at different times (9, 12 and 24 h) after irradiation. Before immunofluorescence protocol cells were permeabilized with PBS supplemented with 0.2% Triton X-100 for 2 min and blocked in PBS-5% BSA for 30 min. Then, cells were incubated with rabbit polyclonal anti-53BP1 (Santa Cruz; 1/1,000) diluted in PBS-1% BSA. After washes with PBS-0.1% Tween 20, cells were incubated with the corresponding Alexa Fluor-conjugated secondary antibody (Jackson; 1/1,000 dilution in 1% BSA-PBS) and washed again. Finally, cells were counterstained with 4,6 diamidino-2-phenylindole (DAPI 1 μg/ml; Sigma) and mounted using Vectashield mounting medium (Vector Laboratories). Samples were visualized using the 488-nm (Alexa 488) and 405-nm (for DAPI) lasers. Highly resolved z-stacks were captured using a Leyca DM6000B fluorescence microscope with a HCX PL APO 63x/NA 1.40 oil immersion objective. Subsequently, 3D rendering was performed to convert the 3D z-stacks into a 2D image, and 53BP1 foci were manually (double-blind) counted. Data represent means of three independent experiments, in which at least 50 cells were counted at each experimental condition.

For proximity ligation assays (PLA) U2OS cells were grown on sterile glass coverslips and transiently transfected with p3xFLAG-Myc-CMV expression vector containing either wild-type POLL or POLL-T204A phospho-blocking mutant cDNAs using Gene Juice (Novagen) according to manufacturer's protocol. After 48 h cells were exposed or not to 2 Gy of IR and allowed to recover for 1 h. Then, cells were fixed and permeabilized as previously described. The PLA assay was performed with the Duolink PLA kit (Sigma) following manufacturer's instructions, and using mouse anti-FLAG M2 (Sigma; 1/5,000) and either rabbit anti-Ku80 (1/1,000; Santa Cruz), rabbit anti-XRCC4 (Santa Cruz; 1/1,000) or rabbit anti-DNA-PKcs (1/1,000; Santa Cruz) primary antibodies. After final wash step cells were counterstained with DAPI and mounted as described above. Samples were visualized using the 594-nm (Alexa 594) and 405-nm (for DAPI) lasers. Highly resolved z-stacks were captured using a Leyca DM6000B fluorescence microscope with a HCX PL APO 63x/NA 1.40 oil immersion

objective. Subsequently, 3D rendering was performed to convert the 3D z-stacks into a 2D image, and PLA foci were manually (double-blind) counted. Data represent means of three independent experiments, in which at least 50 cells were counted at each experimental condition.

2.5 Generation of a phospho-specific antibody to Polλ T204

Antibodies against Polλ phosphorylated at threonine 204 were generated in rabbit using peptides containing phosphorylated threonine 204 (pT204) coupled to KLH according to standard immunization protocols. The phospho-specific antibodies were partially purified from serum by two sequential steps using aldehyde-activated cross-linked beaded agarose columns (Thermo Scientific) coupled to either the synthetic peptides containing non-phosphorylated (npT204) or phosphorylated T204 (pT204) (Thermo Scientific) according to manufacturer's protocol. Antibodies were eluted using 200 mM glycine pH 2.5, neutralized with Tris 1M pH 8 and concentrated with centrifugal filters (Centricon 3,000 NMWL Ultracel YM, Millipore). Partially purified phospho-specific antibodies were pre-incubated for 2 h with non-phosphorylated T204 peptide (10 μg/ml) to block remaining non-phospho specific antibodies, and then used in immunoblotting experiments as described above.

2.6 Kinase assays

Recombinant wild-type Polλ and phospho-blocking mutants (T204A, T188A T188,204A) were over-expressed in *E. coli* BL21-pRIL and purified as previously described [28]. One microgram of purified proteins was used in kinase assays *in vitro* with either 20 units of human DNA-PK complex (Promega) or immunoprecipitated ATM. ATM was immunoprecipitated from 293T cells that were transfected with a plasmid encoding FLAG-tagged ATM (pcDNA3.1(+)Flag-His-ATM wild-type was a gift from Dr. Michael Kastan; Addgene plasmid #31985 [29]). Cells were lysed with lysis buffer (50 mM Tris [pH7.4], 150 mM NaCl, 10% glycerol, 0.2% Tween 20, 0.2% NP40, and 1 mM DTT, protease inhibitors, and phosphatase inhibitors) and FLAG-tagged ATM was immunoprecipitated with anti-FLAG M2 agarose (Sigma-Aldrich) and Protein G-coupled Dynabeads (Life Technologies) as described above. Alternatively, ATM was immunoprecipitated from G361 (ATM-proficient) or HT144 (ATM-deficient) cell lines using anti-ATM antibody (monoclonal Anti-ATM Clone MAT3-4G10/8, Sigma) and Protein G-coupled Dynabeads (Life Technologies) as described above. Kinases assays were performed in kinase reaction buffer (50 mM Tris-HCl pH 7.5, 10 mM MgCl2, 0.1 mM EDTA, 2 mM DTT) supplemented with 200 μM of ATP and double-stranded DNA. Radiolabelling assay was performed in the presence of [γ-^{32}P]-ATP (0.05 μCi/μl; PerkinElmer). All reaction mixtures were incubated at 30°C for 30 min and boiled in Laemmli buffer for 5 min before loading onto 4-20% gradient SDS-PAGE gels (Biorad). Gels were dryed and radioactive proteins detected by phosphor-imaging using a Fuji-gel scanner. Quantification of relative band intensities was carried out using ImageJ software. For kinase assay on peptide-scanning arrays, N-terminal acetylated overlapping dodecapeptides covering the N-terminal domains of human Polλ were generated by automated spot synthesis onto an amino-derivatized cellulose membrane (CNB Proteomics Core Facility, Proteored, Spain). Peptides were immobilized by their C-termini via a polyethylene glycol spacer. Overlapping peptides were spotted onto membrane so that they shared 10 amino acids with its adjacent peptide on the array, corresponding to a change

of two amino acids per peptide. The incubation of the peptide-array with human purified DNA-PKcs (a kind gift from Dr. Susan Lees-Miller) and [γ-^{32}P]-ATP was performed as described above.

2.7 Thermal shift and partial proteolysis assays

For protein thermal shift experiments, purified human Polλ proteins (2 μg each sample) were mixed with PTS-Dye (Applied Biosystems) and melting profiles were obtained within a range of 25–99°C using a ramping rate of 0.05°C s^{-1} and an acquisition of 20 data points per degree celsius in a ViiA™7 Real-Time PCR System (Applied Biosystems). Data was analyzed using the Protein Thermal Shift™ Software v1.0 (Applied Biosystems). Data was corrected for the background signal of the buffer conditions and presented as units of fluorescence with respect to temperature. Melting temperatures (T_m) were determined according to the Boltzmann model. Error bars represent standard deviation from four independent replicates. For proteolysis assays purified human Polλ proteins (5 μg each sample) were incubated at 37°C for 120 min with 0.2 μg trypsin (Promega) in a buffer containing 25 mM MOPS pH 7.0, 20 mM Tris pH 8.0, 5 mM MgCl2, 8% glycerol, 80 mM NaCl and 2 mM DTT. Reactions were stopped by boiling in Laemmli buffer for 5 minutes at 95°C and resolved by 10% SDS-PAGE and Coomassie blue staining.

2.8 DNA polymerization assays

Recombinant wild-type Polλ, phospho-blocking (T204A) and phospho-mimic (T204E) mutants were over-expressed in *E. coli* and purified as previously described [28]. Oligonucleotides used for DNA polymerization assays were purchased from Sigma and purified by 8M urea-20% polyacrylamide gel electrophoresis. Dideoxynucleotides (ddNTPs) and deoxynucleotides (dNTPs) were acquired from GE Healthcare. Oligonucleotides used as primers were 5′-labelled with [γ-^{32}P]-ATP (Perkin-Elmer) and T4 polynucleotide kinase (New England Biolabs). For 1 nt DNA gap-filling assays, a 5′-[^{32}P]-labelled 15-mer DNA primer (5′-GATCACAGTGAGTAC-3′) was hybridized to a 28-mer DNA template (5′-AGAAGTGTATCTCGTACTCACTGTGATC-3′) and to a 12-mer DNA downstream molecule harboring a 5′-phosphate group (5′-AGATACACTTCT-3′). Purified Polλ (50 nM) was incubated with 2.5 nM of the labelled 1 nt gapped DNA in a reaction mixture (20 μl) containing $MgCl_2$ (2.5 mM), increasing concentrations of ddGTP (0.1, 0.25, 0.5, 1, 2.5 nM) and 1x of reaction buffer (50 mM Tris-HCl (pH 7.5), 1 mM DTT, 4% glycerol and 0.1 mg/ml BSA). Given that Polλ does not discriminate between dNTPs and ddNTPs [30], ddNTPs were used for the gap-filling of 1nt-gapped substrates to ensure that polymerization events were restricted to a +1 nt insertion. Following 30 min of incubation at 30°C, reactions were stopped by adding loading buffer (95% (v/v) formamide, 10 mM EDTA, 0.1% (w/v) xylene cyanol and 0.1% (w/v) bromophenol blue) and the products were separated by 8M urea-20% polyacrylamide electrophoresis. After electrophoresis, products of extension were analyzed by autoradiography and gel band intensities determined by densitometry. For *in vitro* NHEJ assays, a 5′-[^{32}P]-labelled 15-mer DNA primer (5′-CCCTCCCTCCGCGGC-3′) was hybridized to a 11-mer DNA oligonucleotide (5′-CGGAGGGAGGG-3′) to generate a labelled primer double stranded DNA molecule with a 3′-overhang. A 21-mer DNA template (5′-CGCGCACTCACGTCCCTCGCC-3′) was hybridized to a 16-mer DNA oligonucleotide (5′-GGGACGTGAGTGCGCG-3′) harboring

a 5′-phosphate group when indicated, to generate a 3′-protruding double stranded DNA template molecule. 5 nM of the labelled primer molecule and 12.5 nM of the template molecule were incubated with purified Polλ (500 nM), $MnCl_2$ (0.1 mM), and either increasing concentrations of dGTP (10, 25, 50, 100 and 500 nM) for efficiency assays or 500 nM of the indicated dNTPs for fidelity assays. In each case, the final reaction volume (20 μl) contained 1X reaction buffer and was incubated at 30°C for 60 min. Reactions were stopped by the addition of loading buffer and extension products were analyzed as described above.

2.9 Extrachromosomal NHEJ repair assay

The extrachromosomal substrate preparation and NHEJ repair assays were carried out as described previously [24]. Briefly, 285-bp linear DNA fragments were generated by PCR amplification with primers 5′-CAAGTGGTCCACCGTCATGGCTTAGCTGTATAG-3′ and 5′-GCCGACCAGCGTCATGGCACACCCATCTCA-3′, digested with BstXI (New England Biolabs) to generate GACG3′ overhangs and purified using a Qiaquick PCR purification kit (Qiagen). This purified substrate (20 ng), together with 600 ng of pMAX-GFP plasmid (Lonza), was introduced into $2x10^5$ Polμ-Polλ double-deficient mouse embryonic fibroblasts (MEFs) in a 10 μl volume by electroporation (Neon, Invitrogen) using a 1350 V-30 ms pulse. Following electroporation, cells were incubated at 37 °C for 1 hour in fresh media, washed with PBS to remove untransfected substrate, and the total cellular DNA was harvested using a QIAamp DNA mini kit (Qiagen). Complementation of the MEF cells with purified proteins were carried out as described above but with the inclusion of 0.1–0.5 ng of purified proteins. Cells lacking both polymerases were used to ensure that all of the products of synthesis could be unambiguously attributed to activity of the introduced protein. Repair accuracy was characterized by PCR amplification of the repair products using Cy-5 labeled PCR primers (5′-CTTACGTTTGATTTCCCTGACTATACAG-3′ and 5′-GCAGGGTAGCCAGTCTGAGATG-3′) and digestion with enzyme AatII (New England Biolabs). Digestion products were resolved on a 5% (wt/vol) native polyacrylamide gel, visualized using a Typhoon Imager (GE Healthcare) and quantified using ImageJ.

3. Results

Our previous results showed that Tel1 phosphorylates yeast PolX polymerase (Pol4) in response to DSB induction, such phosphorylation being relevant for a competent role of Pol4 during NHEJ [31]. In higher eukaryotes, Polλ constitutes the closest ortholog to yeast Pol4 and ATM is the central kinase operating in response to IR-induced DSBs [3]. Therefore, we sought to substantiate the possible conservation of PolX regulation during NHEJ in human cells through an evaluation of Polλ phosphorylation by ATM, a possibility supported by previous proteomic assays [32]. We performed *in vitro* kinase assays using purified Polλ and ATM-enriched immunoprecipitates obtained from human 293T cells transfected with a plasmid encoding FLAG-tagged ATM [29] and using anti-FLAG antibodies (Figure 1A; see Materials and Methods). These assays showed Polλ to be efficiently phosphorylated by the immunoprecipitates *in vitro*, with phosphorylation mainly occurring in the N-terminal region, since a mutant protein lacking the amino terminal BRCT and serine-proline rich domains was barely phosphorylated (Figure 1B). To confirm that ATM was the kinase responsible of the phosphorylation we also performed *in vitro* kinase

assays with immunoprecipitates obtained from cell lines either proficient or deficient in ATM using an anti-ATM antibody (Figure 1C). We found a very similar pattern of Polλ phosphorylation by using both ATM-proficient and ATM-deficient samples, which suggested that other kinase was able to catalyze the reaction (Figure 1D). Since the related PIKK kinase DNA-PKcs, a major player in NHEJ repair, is very abundant in human cells and could be contaminating the immunoprecipitates obtained by using the anti-ATM antibody in low stringent conditions, we evaluated the phosphorylation of human Polλ by DNA-PKcs. We performed kinase assays using purified human Polλ and DNA-PK complex that showed Polλ to be efficiently phosphorylated by DNA-PKcs *in vitro* in the N-terminal region, in agreement with our previous results (Figure 2A). Phosphorylation was undetected in a close homolog of Polλ in human cells, DNA Polymerase β, according to the lack of these N-terminal domains (Figure 2A). Western blot analysis using an antibody specifically recognizing phosphorylated [S/T]Q sites, the consensus sites for DNA-PKcs activity, confirmed human Polλ to be phosphorylated by DNA-PKcs *in vitro* (Figure 2B). This analysis also showed a significant, although not complete, decrease in phosphorylation in the presence of a specific DNA-PKcs inhibitor and a complete absence of phosphorylation following phosphatase treatment (Figure 2B), further confirming the DNA-PKcs mediated activity. Analysis of the amino acid sequence of human Polλ with specialized software for the detection of phosphorylation sites [33] identified four sites matching the [S/T]Q consensus motif common for all PIKKs: T188, T204, S365 and S463. Interestingly, two of these are localized in the N-terminal S/P-rich domain (Figure 2C), which had initially been suggested to be involved in the regulation of Polλ [34], and in which some cyclin-dependent kinase (CDK)-mediated phosphorylations have been identified [35]. [S/T]Q consensus motifs corresponding to T188 and T204 are highly conserved amongst orthologs, particularly in mammals, suggesting their relevance in Polλ function (Figure 2C). To identify the target site for DNA-PKcs mediated phosphorylation of Polλ, we generated phospho-blocking mutant proteins in which these threonine residues were substituted by alanines (Polλ-T188A and Polλ-T204A, respectively), thereby eliminating the corresponding phosphorylation sites. Western blot analysis with [S/T]Q phospho-specific antibodies (Figure 2B) and *in vitro* kinase assays using these purified phospho-blocking mutant proteins (Figure 2D) showed a strong reduction in Polλ-T204A phosphorylation with respect to wild-type protein, indicating that T204 residue was the principal target for DNA-PKcs mediated phosphorylation. *In vitro* kinase assays on a peptide-array of human Polλ covering its N-terminal sequence, including BRCT and S/P-rich domains, also confirmed this finding (Figure 2E). Of note, peptide-array also detected DNA-PKcs mediated phosphorylation sites out of the [S/T]Q consensus motif, which could reflect either non-specific phosphorylatable residues, detected as false positives, or non-consensus sites for DNA-PKcs phosphorylation. Taken together, these results demonstrate that human Polλ can be phosphorylated *in vitro* by both ATM and DNA-PKcs, with T204 being arguably the main target for such modification.

Given the role of Polλ in NHEJ and the newly identified phosphorylation at T204 residue, we proceeded to investigate if such phosphorylation occurs *in vivo*. To determine this, we generated rabbit polyclonal antibodies against phosphorylated T204, from which phospho-specific antibodies were partially purified. Phospho-specific enriched antibodies (pT204)

preferentially detected Polλ T204 phosphorylation as demonstrated by using either purified peptides (Figure 3A) or purified Polλ after *in vitro* kinase assays with DNA-PKcs (Figure 3B). Importantly, this pT204 antibody was also able to detect T204 phosphorylation *in vivo* in protein extracts obtained from 293T cells overexpressing FLAG-Polλ subjected to ionizing radiation (IR) (Figure 3C). However, T204 phosphorylation was undetectable in non-irradiated cells or when cells overexpressed the phospho-blocking FLAG-Polλ T204A mutant protein (Figure 3C). All these results validated our phospho-specific antibody to be used in the detection of T204 phosphorylation *in vivo*. Accordingly, we analyzed T204 phosphorylation in a time course experiment after DSB induction with IR. Human 293T cells overexpressing FLAG-tagged Polλ were left untreated or treated with IR and collected at different times after DSB induction. Protein extracts were analyzed by Western blotting with the pT204 antibody, which confirmed that Polλ phosphorylation at T204 residue was triggered *in vivo* in response to DSB induction (Figure 3D). In agreement with this result, slower-migrating form(s) of FLAG-Polλ, which represented phosphorylated Polλ, became more abundant shortly after irradiation (Figure 3D). It should be noted that a fraction of Polλ was already phosphorylated in the absence of irradiation, in agreement with the fact that Polλ can also be phosphorylated by other kinases [35]. To determine whether ATM and/or DNA-PKcs were involved in Polλ T204 phosphorylation after IR-induced DSBs we pre-treated cells with specific inhibitors of DNA-PKcs (NU7441, DNA-PKi) or ATM (KU55933, ATMi) and then analyzed the effect of such treatment on T204 phosphorylation one hour after DSB induction (Figure 3E). Whereas pre-incubation with DNA-PKi had apparently no effect, ATMi severely reduced T204 phosphorylation triggered by IR, indicating that DSB-induced phosphorylation of Polλ *in vivo* was mainly mediated by ATM. This result was corroborated in a time course experiment in which cells were pre-treated with ATMi and/or DNA-PKi (either independently or together), subjected to IR and finally analyzed by immunoblotting to detect T204 phosphorylation at several times after DSB induction (Figure 3F and 3G). As shown in Figure 3F, this analysis confirmed the strong inhibitory effect of ATMi treatment on T204 phosphorylation (Figure 3F and 3G). In the presence of ATMi alone or both inhibitors together T204 phosphorylation was almost undetected until 12 h after irradiation, and became evident 24 h after irradiation (Figure 3F and 3G). On the contrary, the treatment with DNA-PKi had no apparent effect on T204 phosphorylation. Collectively, these results demonstrate that following DSB induction *in vivo* human Polλ is phosphorylated at T204 principally by ATM.

Having demonstrated that Polλ is phosphorylated at T204 after DSB induction *in vivo* we then sought to determine the physiological role of this phosphorylation during NHEJ by analyzing the effect of the phospho-blocking T204A mutation. To rule out any defects in the catalytic activity of the polymerase due to the T204A mutation, we first assayed such activity *in vitro* using purified wild-type and phospho-blocking mutant DNA polymerases (Figure 4). Both proteins showed similar DNA polymerization activity on gapped DNA substrates (Figure 4A) and NHEJ substrates resembling those preferentially managed by Polλ *in vivo* (Figure 4B) [24], indicating that the mutation does not have deleterious effects on the catalytic activity of Polλ. Conversely, *in vitro* polymerization activity of a mutant protein in which T204 residue was changed to a glutamic acid residue (T204E), trying to mimic phosphorylation modification, showed a decreased DNA polymerization activity *in*

vitro, especially in NHEJ reactions (Figure 4). Since T204 residue is far from the catalytic center of Polλ, this result suggested a defect in the global conformation of T204E mutant protein in solution with respect to wild-type Polλ, which was supported by thermal shift and partial proteolysis assays (Supplemental Figure 1A and 1B). The fidelity of the polymerization reactions carried out by all the proteins and the strict requirement for downstream 5′-phosphate groups in the gapped DNA molecules used in the assays were similar (Figure 4C).

We next analyzed the sensitivity of cells deficient in Polλ to IR-induced DSBs. Since POLL deficient cells are only mildly sensitive to IR [24], survival assays in response to IR were not suitable for this purpose. Consequently, we decided to analyze the time course of 53BP1 foci disappearance after DSB induction with a high dose of IR, in order to generate DSBs with complex DNA ends that would require some processing, likely including DNA gap-filling synthesis, before ligation. 53BP1 is an important positive regulator of NHEJ-mediated DSB repair and, given that the number of 53BP1 foci correlates well with the number of breaks [36,37], their quantification following DSB induction constitutes a well-established procedure in the monitoring of the NHEJ repair process *in vivo*. Time course experiments were performed in human U2OS cells depleted or not of endogenous Polλ by using siRNA (Figure 5A and 5B). Under these experimental conditions, the number of 53BP1 foci observed in Polλ-depleted cells was significantly higher than that observed in cells expressing a control luciferase siRNA in all analyzed conditions after irradiation (Figure 5B and 5C), indicating that the absence of Polλ results in a defect in the repair of IR-induced DSBs. Since IR produces a wide variety of DNA ends at the breaks, not all requiring Polλ activity for repair, we sought to determine the role of T204 phosphorylation in the repair of DSBs by using an experimental assay leading to more homogeneous DSBs. We took advantage of a recently described cellular assay to specifically measure Polλ-dependent repair of a defined DNA end structure *in vivo* (Figure 6A) [24]. According to the specialization of Polλ for filling gaps longer than 1 nt during NHEJ, DNA ends that align to generate a 2 nt gap substrate are repaired by less accurate polymerase-independent means in MEF cells deficient in both Polλ and Polμ, and the ability to perform accurate repair is recovered upon complementation with wild-type Polλ (Figure 6B) [24]. We first complemented MEFs deficient in these polymerases with increasing amounts of wild-type Polλ to identify levels of Polλ that were sub-saturating (Figure 6B) [24], and then determined that when assessed under these conditions, the Polλ-T204A phospho-blocking mutant protein was 3-fold less effective than the wild-type Polλ in complementation of these deficient MEFs (Figures 6B and 6C). Given that T204A mutation was not disadvantageous for Polλ DNA synthesis capability *in vitro*, these results indicate that T204 availability can be required for an efficient Polλ-dependent gap-filling DNA synthesis during the NHEJ repair *in vivo*.

To gain further insight into the molecular role of T204 phosphorylation during NHEJ we investigated the protein-protein interactions between Polλ and NHEJ core factors. Recent proteomic analyses have identified both Ku80 and DNA-PKcs as the principal partners of Polλ in human cells [38], a finding in agreement with the interaction of Polλ with Ku:DNA complexes *in vitro* [20,23]. We performed immunoprecipitation (IP) assays using anti-FLAG antibody and 293T cells overexpressing FLAG-Polλ that had previously been subjected or

not IR-induced DSBs. Treatment with the broad-spectrum nuclease benzonase was included during the immunoprecipitation to rule out bridging of these proteins by DNA. As shown in Figure 7A, an efficient co-precipitation of both Ku80 or DNA-PKcs together with FLAG-Polλ could be observed both in irradiated and non-irradiated cells, indicating their interaction *in vivo*. Notably, the interaction of Polλ with Ku80 or DNA-PKcs was very specific, since other NHEJ factor such as XRCC4 did not precipitate in the same experimental conditions (Figure 7A). Although it has been reported that the BRCT domain is the essential domain for human Polλ interaction with the Ku complex *in vitro* [20,23], the analysis of such interaction using different deletion mutants of Polλ in the absence of DNA indicated that the presence of the S/P-rich domain was also a requirement for an efficient Polλ-Ku80 association (Figure 7B). Proximity ligation assays (PLA) in human U2OS cells confirmed the interactions detected by co-immunoprecipitation in more physiological conditions (Figure 7C). We also used these PLA assays to analyze the putative effect of Polλ-T204A mutation on the interaction with Ku80, representative of DNA-PK complex, in response to IR-induced DSBs. We detected robust PLA signals of Ku80 and Polλ in cells in the absence of irradiation, in agreement with previous co-immunoprecipitation results (Figure 7D). In these experimental conditions, PLA signals were similar in cells overexpressing either wild-type Polλ or Polλ-T204A (Figure 7D). Interestingly, following DSB induction, we observed a significant decrease (around 15%) in the co-localization of Ku80 and Polλ specifically in cells overexpressing Polλ-T204A, but not in those overexpressing wild-type Polλ (Figure 7D). Overall, these results indicate that T204 phosphorylation is important in the maintenance of Ku80-Polλ association after DBSs *in vivo* and support its relevance for optimal NHEJ repair.

4. Discussion

In response to DNA DSBs hundreds of proteins are phosphorylated by PIKK kinases ATM and DNA-PKcs. ATM is a key transducer of the DSB response [3] and DNA-PKcs is a major player in the regulation of NHEJ process [39], the principal pathway to repair DSBs in human cells [4]. Paradoxically, despite compelling evidence demonstrating that many NHEJ factors are phosphorylated by ATM and/or DNA-PKcs both *in vitro* and after DSBs induction *in vivo* [11-14], only a few of these post-translational modifications have been demonstrated to be functionally relevant for NHEJ process [14-18,39]. In the present study, we gained insight into the NHEJ mechanism by describing a novel regulation of human Polλ by ATM-mediated phosphorylation. We show that human Polλ is required for the repair of IR-induced DSBs *in vivo* and that Polλ phosphorylation may facilitate Polλ-mediated gap-filling DNA synthesis during NHEJ.

We have identified threonine 204 (T204) as the main target in Polλ for ATM/DNA-PKcs dependent phosphorylation *in vitro*. This residue is located in a serine-proline rich (S/P-rich) region that acts as a linker between the independent globular modules formed by N-terminal BRCT and C-terminal catalytic domains [22]. S/P-rich region had initially been suggested as acting as a regulation domain target for post-translational modifications [34], and, indeed, contains residues that are phosphorylated by cyclin-dependent kinases [35]. Our *in vitro* kinase assays have also detected DNA-PKcs phosphorylation sites in the S/P-rich region not having the [S/T]Q consensus motif. Thus, some of the peptides containing the two

consecutive Ser residues S42 and S43, and some of those containing T221, S222 and/or S230 can be also targeted by DNA-PKcs *in vitro*. This could be a consequence of the particular abundance in serine/threonine residues of this region, which, when followed by hydrophobic amino acids, can also be targeted by DNA-PKcs, as reported in other NHEJ factors [11,12,39,40]. Further studies will be required to assess the impact of the putative phosphorylation at these non-consensus sites in Polλ function. Although different crystal structures of human Polλ have been resolved [25,41], the S/P-rich domain is not included, probably due to its high degree of flexibility or disordered nature. Intrinsically disordered regions do not form fixed structures under physiological conditions, and carry out important regulatory functions [42]. The presence of phosphorylation sites in these flexible regions is common among NHEJ proteins, probably due to the fact that such flexibility facilitates their access to the active site of large kinases such as ATM or DNA-PKcs [43-45]. On the basis of its location, it can be hypothesized that Polλ T204 phosphorylation could generate protein conformational changes relevant to either its recruitment to DSBs or its assembly with DNA-bound DNA-PK complex during NHEJ repair process. In agreement to this second possibility, we have detected a solid interaction between Polλ and DNA-PKcs or Ku80, which is also corroborated by recent proteomic analyses [38]. The regulation of Polλ-DNA-PK interaction at DSBs through Polλ phosphorylation would be useful and in agreement with the pivotal role of DNA-PK complex in the coordination of NHEJ process conforming to specific DNA end configurations [46]. In an attempt to address the conformational change hypothesis we characterized the phospho-mimetic mutant Polλ T204E. Both thermal shift and partial proteolysis assays indicate that T204E mutation modifies Polλ global conformation. We observed that this mutation causes a decrease in the activity of Polλ using NHEJ substrates *in vivo* (Supplemental Figure 1C), which is in contrast with results indicating that T204 phosphorylation stimulates NHEJ and DSB repair *in vivo*. Since the T204E mutation causes a similar defect in NHEJ assays *in vitro,* where only the protein and DNA substrates are present, it is not possible to discriminate if the mutation is mimicking phosphorylation modification *in vivo* or not, and the results obtained with T204E mutant are not very conclusive. In any case, they do reinforce the relevance of modifications affecting T204 amino acid residue to modulate the activity of Polλ during NHEJ. Further structural analysis would help to clarify this point.

Despite the fact that Polλ/DNA-PK association is also detected in the absence of DSB induction, we have observed that Polλ T204A phospho-blocking mutant protein displays a significant defect in its association with Ku80 specifically when DSBs are induced with IR. Although the defect is relatively mild, it cannot be ruled out the effect of strong overexpression of Polλ proteins in our experiments, that could be to some extent masking the real effects of mutation. In any case, the slight reduction in the Polλ/DNA-PK interaction caused by the phospho-blocking mutation T204A may reflect the fact that the participation of Polλ can be restricted to the repair of a specific subset of DNA end configurations, according with its substrate specificity [24]. This could also explain why Polλ defective cells are not highly sensitive to IR [24]. Comparable defects have been reported in other proteins, such as ATM kinase itself or Artemis nuclease, that specifically participate in the repair of a fraction of DSBs generated by IR, shown to be linked to heterochromatic regions (HC-DSBs) [47-50]. In this context, ATM activation is necessary to

phosphorylate some substrates like H2AX or KAP1, which would relax chromatin compaction allowing the access of repair proteins to HC-DSBs [47,48]. Another possible scenario is the repair of blocked DNA ends, that also requires specifically the activity of ATM [51]. According to our results, phosphorylation of Polλ at T204 residue *in vivo* strictly requires ATM activity and may facilitate NHEJ repair. The novel functional interaction between ATM and Polλ in the response to IR-induced DSBs suggests a participation of Polλ in the repair of some of these specially difficult to repair DSBs. Future studies examining the impact of Polλ and its ATM-mediated phosphorylation with HC-DSBs or blocked DSBs will be required to consolidate these findings.

Our work shows that Polλ T204 phosphorylation may fluctuate and is principally regulated by ATM in time after DSB induction. Our assays show that whereas T204 phosphorylation after IR-induced DSBs is dramatically reduced in the presence of an ATM inhibitor, this decrease does not occur in the presence of a DNA-PKcs inhibitor. This is in contrast with our results *in vitro* showing the efficient phosphorylation of Polλ either using ATM-deficient protein extracts or directly purified DNA-PKcs, that would fit well with a role of Polλ in canonical NHEJ [8,23,24,26]. Of note, it is possible, but difficult to be measured, a degree of functional redundancy of phosphorylation by ATM and DNA-PKcs *in vivo*, as occurs in other NHEJ factors [13,14], including DNA-PKcs itself [39], or in apical proteins during the DDR [52,53]. In addition, it is worth noting that the lower contribution of DNA-PKcs to Polλ phosphorylation observed *in vivo* after IR-induced DSBs could be underestimated due to the crosstalk between ATM and DNA-PKcs [53,54] and the compensation effects that may appear to preserve genomic integrity, which are also difficult to measure. In this regard, it has been recently reported how the loss of DNA-PKcs function by the use of specific inhibitors leads to hyper-activation of ATM [55]. On the other hand, the strong decrease of T204 phosphorylation generated by ATM inhibitor could be not only caused by direct inhibition of ATM kinase activity, but also due to a collateral effect on the activity of DNA-PKcs, one of the targets of ATM after IR-induced DSBs [54]. In any case, after the treatment with the ATM inhibitor alone we observe that T204 phosphorylation strongly increases at late times after IR-induced DSBs, in agreement with the fact that inhibition of ATM retards repair of the chemically complex DSBs that require DNA-PKcs [56]. Intriguingly, when we used both ATM and DNA-PKcs specific inhibitors together, we could observe a similar effect in T204 phosphorylation at late times after IR-induced DSBs. A plausible explanation is the possible participation of the third DDR-related PIKKs, ATR, which might compensate the lack of the activity of the other two kinases. According with such a possibility, it has been reported that ATR kinase activity can be important for survival after IR in G1 phase cells, in which it could contribute to DSB repair in the absence of homologous recombination repair [57]. By integrating our results with previous findings suggesting distinct NHEJ sub-pathways to repair different types of DSBs with different levels of complexity and complementarity at their ends [23,24,53,56,58], we propose a model in which phosphorylation of Polλ by ATM facilitates Polλ recruitment to a subset of DNA-PK bound DSBs, thereby avoiding superfluous competition with other NHEJ polymerases (Figure 8). This might be postulated as a way to make highly accurate Polλ the first choice to repair DSBs having clean and complementary ends with the minimal loss of genetic information [24]. ATM-mediated phosphorylation of Polλ could be also required for those

complex DSBs whose repair has been shown to be completely dependent on ATM activity [47-51] (Figure 8). Of note, if ATM is not able to phosphorylate Polλ, DNA-PKcs might perform such reaction at the breaks, resulting in the same biological effect (Figure 8). Future work will be required to address the precise role and relative contribution of ATM and DNA-PKcs to the regulation of Polλ mediated by phosphorylation at its T204 residue, likely a complex task taking into account the functional interplay of both kinases.

In summary, our findings provide important insight into how human Polλ is regulated by ATM after IR-mediated DSB induction and clearly indicates that the phosphorylation of Polλ at T204 is undeniably beneficial for DSB repair *in vivo*. Phosphorylation-dependent enhancement of Polλ activity possibly occurs through conformational changes of the protein that favor its interaction with other NHEJ proteins at a specific subset of DNA end configurations, according to its substrate specificities.

Supplementary Material

Refer to Web version on PubMed Central for supplementary material.

Acknowledgments

We thank Dr. S. Lees-Miller for her kind gift of purified human DNA-PKcs, Dr. Y. Shiloh for G361 and HT144 cell lines, Dr. Michael Kastan for pcDNA3.1(+)Flag-His-ATM plasmid, Dr. F. Gómez-Herreros and Dr. Belén Gómez-González for their feedback on the manuscript and useful discussions, and M. Simon for style revision.

Funding: This work was supported by grants from the Spanish Ministry of Economy and Competitiveness (MINECO) and the European Commission (European Regional Development Fund) to J.F.R. (RYC-2011-08752, BFU2013-44343-P) and to F.C-L. (SAF2014-55532-R). J.F.R. was the recipient of a Ramón y Cajal contract from the Spanish Ministry of Economy and Competitiveness (MINECO). G.S.-M. was supported by a JAE-predoctoral fellowship from the Spanish Research Council (CSIC). Work by J.M.P in the Ramsden laboratory was supported by a postdoctoral fellowship from the American Cancer Society (PF-14-0438-01-DMC) and an NCI grant (CA097096) to D.A.R.

References

1. Phillips ER, McKinnon PJ. DNA double-strand break repair and development. Oncogene. 2007; 26:7799–7808. DOI: 10.1038/sj.onc.1210877 [PubMed: 18066093]
2. Jackson SP, Bartek J. The DNA-damage response in human biology and disease. Nature. 2009; 461:1071–1078. DOI: 10.1038/nature08467 [PubMed: 19847258]
3. Shiloh Y, Ziv Y. The ATM protein kinase: regulating the cellular response togenotoxic stress, and more. Nat Rev Mol Cell Biol. 2013; 14:197–210. DOI: 10.1038/nrm3546
4. Karanam K, Kafri R, Loewer A, Lahav G. Quantitative live cell imaging reveals a gradual shift between DNA repair mechanisms and a maximal use of HR in mid S phase. Mol Cell. 2012; 47:320–329. DOI: 10.1016/j.molcel.2012.05.052 [PubMed: 22841003]
5. Ghezraoui H, Piganeau M, Renouf B, Renaud JB, Sallmyr A, Ruis B, Oh S, Tomkinson AE, Hendrickson EA, Giovannangeli C, Jasin M, Brunet E. Chromosomal translocations in human cells are generated by canonical nonhomologous end-joining. Mol Cell. 2014; 55:829–842. DOI: 10.1016/j.molcel.2014.08.002 [PubMed: 25201414]
6. Waters CA, Strande NT, Wyatt DW, Pryor JM, Ramsden DA. Nonhomologous end joining: a good solution for bad ends. DNA Repair (Amst). 2014; 17:39–51. DOI: 10.1016/j.dnarep.2014.02.008 [PubMed: 24630899]
7. Andres SN, Schellenberg MJ, Wallace BD, Tumbale P, Williams RS. Recognition and repair of chemically heterogeneous structures at DNA ends. Environ Mol Mutagen. 2015; 56:1–21. DOI: 10.1002/em.21892 [PubMed: 25111769]

8. Lieber MR, Lu H, Gu J, Schwarz K. Flexibility in the order of action and in the enzymology of the nuclease, polymerases, and ligase of vertebrate nonhomologous DNA end joining: relevance to cancer, aging, and the immune system. Cell Res. 2008; 18:125–133. DOI: 10.1038/cr.2007.108 [PubMed: 18087292]
9. Downs JA, Jackson SP. A means to a DNA end: the many roles of Ku. Nat Rev Mol Cell Biol. 2004; 5:367–378. DOI: 10.1038/nrm1367 [PubMed: 15122350]
10. Singleton BK, Torres-Arzayus MI, Rottinghaus ST, Taccioli GE, Jeggo PA. The C terminus of Ku80 activates the DNA-dependent protein kinase catalytic subunit. Mol Cell Biol. 1999; 19:3267–3277. DOI: 10.1128/MCB.19.5.3267 [PubMed: 10207052]
11. Mahaney BL, Meek K, Lees-Miller SP. Repair of ionizing radiation-induced DNA double-strand breaks by non-homologous end-joining. Biochemical J. 2009; 417:639–650. DOI: 10.1042/BJ20080413
12. Yu Y, Wang W, Ding Q, Ye R, Chen D, Merkle D, Schriemer D, Meek K, Lees-Miller SP. DNA-PK phosphorylation sites in XRCC4 are not required for survival after radiation or for V(D)J recombination. DNA Repair (Amst). 2003; 2:1239–1252. DOI: 10.1016/S1568-7864(03)00143-5 [PubMed: 14599745]
13. Douglas P, Gupta S, Morrice N, Meek K, Lees-Miller SP. DNA-PK-dependent phosphorylation of Ku70/80 is not required for non-homologous end joining. DNA Repair (Amst). 2005; 4:1006–1018. DOI: 10.1016/j.dnarep.2005.05.003 [PubMed: 15941674]
14. Yu Y, Mahaney BL, Yano K, Ye R, Fang S, Douglas P, Chen DJ, Lees-Miller SP. DNA-PK and ATM phosphorylation sites in XLF/Cernunnos are not required for repair of DNA double strand breaks. DNA Repair (Amst). 2008; 7:1680–1692. DOI: 10.1016/j.dnarep.2008.06.015 [PubMed: 18644470]
15. Chan DW, Chen BP, Prithivirajsingh S, Kurimasa A, Story MD, Qin J, Chen DJ. Autophosphorylation of the DNA-dependent protein kinase catalytic subunit is required for rejoining of DNA double-strand breaks. Genes Dev. 2002; 16:2333–2338. DOI: 10.1101/gad.1015202 [PubMed: 12231622]
16. Ding Q, Reddy YV, Wang W, Woods T, Douglas P, Ramsden DA, Lees-Miller SP, Meek K. Autophosphorylation of the catalytic subunit of the DNA-dependent protein kinase is required for efficient end processing during DNA double-strand break repair. Mol Cell Biol. 2003; 23:5836–5848. DOI: 10.1128/MCB.23.16.5836-5848.2003 [PubMed: 12897153]
17. Reddy YV, Ding Q, Lees-Miller SP, Meek K, Ramsden DA. Non-homologous end joining requires that the DNA-PK complex undergo an autophosphorylation-dependent rearrangement at DNA ends. J Biol Chem. 2004; 279:39408–39413. DOI: 10.1074/jbc.M406432200 [PubMed: 15258142]
18. Cui X, Yu Y, Gupta S, Cho YM, Lees-Miller SP, Meek K. Autophosphorylation of DNA-dependent protein kinase regulates DNA end processing and may also alter double-strand break repair pathway choice. Mol Cell Biol. 2005; 25:10842–10852. DOI: 10.1128/MCB.25.24.10842-10852.2005 [PubMed: 16314509]
19. Uematsu N, Weterings E, Yano K, Morotomi-Yano K, Jakob B, Taucher-Scholz G, Mari PO, van Gent DC, Chen BP, Chen DJ. Autophosphorylation of DNA-PKcs regulates its dynamics at DNA double-strand breaks. J Cell Biol. 2007; 177:219–229. DOI: 10.1083/jcb.200608077 [PubMed: 17438073]
20. Ma Y, Lu H, Tippin B, Goodman MF, Shimazaki N, Koiwai O, Hsieh CL, Schwarz K, Lieber MR. A biochemically defined system for mammalian nonhomologous DNA end joining. Mol Cell. 2004; 16:701–713. DOI: 10.1016/j.molcel.2004.11.017 [PubMed: 15574326]
21. Mahajan KN, Nick Mc Elhinny SA, Mitchell BS, Ramsden DA. Association of DNA polymerase mu (pol mu) with Ku and ligase IV: role for pol mu in end-joining double-strand break repair. Mol Cell Biol. 2002; 22:5194–5202. DOI: 10.1128/MCB.22.14.5194-5202.2002 [PubMed: 12077346]
22. Garcia-Diaz M, Bebenek K, Gao G, Pedersen LC, London RE, Kunkel TA. Structure-function studies of DNA polymerase lambda. DNA Repair (Amst). 2005; 4:1358–1367. DOI: 10.1016/j.dnarep.2005.09.001 [PubMed: 16213194]
23. Nick Mc Elhinny SA, Havener JM, Garcia-Diaz M, Juárez R, Bebenek K, Kee BL, Blanco L, Kunkel TA, Ramsden DA. A gradient of template dependence defines distinct biological roles for

family X polymerases in nonhomologous end joining. Mol Cell. 2005; 19:357–366. DOI: 10.1016/j.molcel.2005.06.012 [PubMed: 16061182]

24. Pryor JM, Waters CA, Aza A, Asagoshi K, Strom C, Mieczkowski PA, Blanco L, Ramsden DA. Essential role for polymerase specialization in cellular nonhomologous end joining. Proc Natl Acad Sci USA. 2015; 112:E4537–4545. DOI: 10.1073/pnas.1505805112 [PubMed: 26240371]
25. Garcia-Diaz M, Bebenek K, Larrea AA, Havener JM, Perera L, Krahn JM, Pedersen LC, Ramsden DA, Kunkel TA. Template strand scrunching during DNA gap repair synthesis by human polymerase lambda. Nat Struct Mol Biol. 2009; 16:967–972. DOI: 10.1038/nsmb.1654 [PubMed: 19701199]
26. Bertocci B, De Smet A, Weill JC, Reynaud CA. Nonoverlapping functions of DNA polymerases mu, lambda, and terminal deoxynucleotidyltransferase during immunoglobulin V(D)J recombination in vivo. Immunity. 2006; 25:31–41. DOI: 10.1016/j.immuni.2006.04.013 [PubMed: 16860755]
27. Zucca E, Bertoletti F, Wimmer U, Ferrari E, Mazzini G, Khoronenkova S, Grosse N, van Loon B, Dianov G, Hübscher U, Maga G. Silencing of human Polλ causes replication stress and is synthetically lethal with an impaired S phase checkpoint. Nucleic Acids Res. 2012; 41:229–241. DOI: 10.1093/nar/gks1016 [PubMed: 23118481]
28. Martin MJ, Garcia-Ortiz MV, Gomez-Bedoya A, Esteban V, Guerra S, Blanco L. (2013) A specific N-terminal extension of the 8 kDa domain is required for DNA end-bridging by human Polμ and Polλ. Nucleic Acids Res. 2013; 41:9105–9116. DOI: 10.1093/nar/gkt681 [PubMed: 23935073]
29. Canman CE, Lim DS, Cimprich KA, Taya Y, Tamai K, Sakaguchi K, Appella E, Kastan MB, Siliciano JD. Activation of the ATM kinase by ionizing radiation and phosphorylation of p53. Science. 1998; 281:1677–1679. DOI: 10.1126/science.281.5383.1677 [PubMed: 9733515]
30. García-Díaz M, Bebenek K, Sabariegos R, Domínguez O, Rodríguez J, Kirchhoff T, García-Palomero E, Picher AJ, Juárez R, Ruiz JF, Kunkel TA, Blanco L. DNA polymerase lambda, a novel DNA repair enzyme in human cells. J Biol Chem. 2002; 277:13184–13191. DOI: 10.1074/jbc.M111601200 [PubMed: 11821417]
31. Ruiz JF, Pardo B, Sastre-Moreno G, Aguilera A, Blanco L. Yeast pol4 promotes tel1-regulated chromosomal translocations. PLoS Genet. 2013; 9:e1003656.doi: 10.1371/journal.pgen.1003656 [PubMed: 23874240]
32. Matsuoka S, Ballif BA, Smogorzewska A, McDonald ER, Hurov KE, Luo J, Bakalarski CE, Zhao Z, Solimini N, Lerenthal Y, Shiloh Y, Gygi SP, Elledge SJ. ATM and ATR substrate analysis reveals extensive protein networks responsive to DNA damage. Science. 2007; 316:1160–1166. DOI: 10.1126/science.1140321 [PubMed: 17525332]
33. Obenauer JC, Cantley LC, Yaffe MB. 2.0: Proteome-wide prediction of cell signaling interactions using short sequence motifs. Nucleic Acids Res. 2003; 31:3635–3641. DOI: 10.1093/nar/gkg58 [PubMed: 12824383]
34. García-Díaz M, Domínguez O, López-Fernández LA, de Lera TL, Saníger ML, Ruiz JF, Párraga M, García-Ortiz MJ, Kirchhoff T, del Mazo J, Bernad A, Blanco L. DNA polymerase lambda (Pol lambda), a novel eukaryotic DNA polymerase with a potential role in meiosis. J Mol Biol. 2000; 301:851–867. DOI: 10.1006/jmbi.2000.4005 [PubMed: 10966791]
35. Frouin I, Toueille M, Ferrari E, Shevelev I, Hübscher U. Phosphorylation of human DNA polymerase lambda by the cyclin-dependent kinase Cdk2/cyclin A complex is modulated by its association with proliferating cell nuclear antigen. Nucleic Acids Res. 2005; 33:5354–5361. DOI: 10.1093/nar/gki845 [PubMed: 16174846]
36. Schultz LB, Chehab NH, Malikzay A, Halazonetis TD. p53 binding protein 1 (53BP1) is an early participant in the cellular response to DNA double-strand breaks. J Cell Biol. 2000; 1381:1381–1390. DOI: 10.1083/jcb.151.7
37. Anderson L, Henderson C, Adachi Y. Phosphorylation and rapid relocalization of 53BP1 to nuclear foci upon DNA damage. Mol Cell Biol. 2001; 21:1719–1729. DOI: 10.1128/MCB.21.5.1719-1729.2001 [PubMed: 11238909]
38. Xing M, Yang M, Huo W, Feng F, Wei L, Jiang W, Ning S, Yan Z, Li W, Wang Q, Hou M, Dong C, Guo R, Gao G, Ji J, Zha S, Lan L, Liang H, Xu D. Interactome analysis identifies a new paralogue of XRCC4 in non-homologous end joining DNA repair pathway. Nat Commun. 2015; 6:6233.doi: 10.1038/ncomms7233 [PubMed: 25670504]

39. Meek K, Dang V, Lees-Miller SP. DNA-PK: the means to justify the ends? Advances in Immunology. 2008; 99:33–58. DOI: 10.1016/S0065-2776(08)00602-0 [PubMed: 19117531]
40. Chan DW, Ye R, Veillette CJ, Lees-Miller SP. DNA-dependent protein kinase phosphorylation sites in Ku 70/80 heterodimer. Biochemistry. 1999; 38:1819–1828. DOI: 10.1021/bi982584b [PubMed: 10026262]
41. Garcia-Diaz M, Bebenek K, Krahn JM, Blanco L, Kunkel TA, Pedersen LC. A structural solution for the DNA polymerase lambda-dependent repair of DNA gaps with minimal homology. Mol Cell. 2004; 13:561–572. DOI: 10.1016/S1097-2765(04)00061-9 [PubMed: 14992725]
42. Sickmeier M, Hamilton JA, LeGall T, Vacic V, Cortese MS, Tantos A, Szabo B, Tompa P, Chen J, Uversky VN, Obradovic Z, Dunker AK. DisProt: the Database of Disordered Proteins. Nucleic Acids Res. 2007; 35:D786–93. DOI: 10.1093/nar/gkl893 [PubMed: 17145717]
43. Zhang Z, Hu W, Cano L, Lee TD, Chen DJ, Chen Y. Solution structure of the C-terminal domain of Ku80 suggests important sites for protein-protein interactions. Structure. 2004; 12:495–502. DOI: 10.1016/j.str.2004.02.007 [PubMed: 15016365]
44. Harris R, Esposito D, Sankar A, Maman JD, Hinks JA, Pearl LH, Driscoll PC. The 3D solution structure of the C-terminal region of Ku86 (Ku86CTR). J Mol Biol. 2004; 335:573–582. DOI: 10.1016/j.jmb.2003.10.047 [PubMed: 14672664]
45. Neal JA, Sugiman-Marangos S, VanderVere-Carozza P, Wagner M, Turchi M, Lees-Miller SP, Junop MS, Meek K. Unraveling the complexities of DNA-dependent protein kinase autophosphorylation. Mol Cell Biol. 2014; 34:2162–2175. DOI: 10.1128/MCB.01554-13 [PubMed: 24687855]
46. Woods DS, Sears CR, Turchi JJ. Recognition of DNA Termini by the C-Terminal Region of the Ku80 and the DNA-Dependent Protein Kinase Catalytic Subunit. PLoS ONE. 2015; 10:e0127321.doi: 10.1371/journal.pone.0127321 [PubMed: 25978375]
47. Riballo E, Kühne M, Rief N, Doherty A, Smith GC, Recio MJ, Reis C, Dahm K, Fricke A, Krempler A, Parker AR, Jackson SP, Gennery A, Jeggo PA, Löbrich M. A pathway of double-strand break rejoining dependent upon ATM, Artemis, and proteins locating to gamma-H2AX foci. Mol Cell. 2004; 16:715–724. DOI: 10.1016/j.molcel.2004.10.029 [PubMed: 15574327]
48. Goodarzi AA, Noon AT, Deckbar D, Ziv Y, Shiloh Y, Löbrich M, Jeggo PA. ATM signaling facilitates repair of DNA double-strand breaks associated with heterochromatin. Mol Cell. 2008; 31:167–77. DOI: 10.1016/j.molcel.2008.05.017 [PubMed: 18657500]
49. Goodarzi AA, Yu Y, Riballo E, Douglas P, Walker SA, Ye R, Härer C, Marchetti C, Morrice N, Jeggo PA, Lees-Miller SP. DNA-PK autophosphorylation facilitates Artemis endonuclease activity. EMBO J. 2006; 25:3880–3889. DOI: 10.1038/sj.emboj7601255 [PubMed: 16874298]
50. Wang J, Pluth JM, Cooper PK, Cowan MJ, Chen DJ, Yannone SM. Artemis deficiency confers a DNA double-strand break repair defect and Artemis phosphorylation status is altered by DNA damage and cell cycle progression. DNA Repair (Amst). 2005; 4:556–570. DOI: 10.1016/j.dnarep.2005.02.001 [PubMed: 15811628]
51. Álvarez-Quilón A, Serrano-Benítez A, Lieberman JA, Quintero C, Sánchez-Gutiérrez D, Escudero LM, Cortés-Ledesma F. ATM specifically mediates repair of double-strand breaks with blocked DNA ends. Nat Commun. 2014; 5:3347.doi: 10.1038/ncomms4347 [PubMed: 24572510]
52. Stiff T, O'Driscoll M, Rief N, Iwabuchi K, Löbrich M, Jeggo PA. ATM and DNA-PK Function Redundantly to Phosphorylate H2AX after Exposure to Ionizing Radiation. Cancer Res. 2004; 64:2390–2396. DOI: 10.1158/0008-5472.CAN-03-3207 [PubMed: 15059890]
53. Callén E, Jankovic M, Wong N, Zha S, Chen HT, Difilippantonio S, Di Virgilio M, Heidkamp G, Alt FW, Nussenzweig A, Nussenzweig M. Essential role for DNA-PKcs in DNA double-strand break repair and apoptosis in ATM-deficient lymphocytes. Mol Cell. 2009; 34:285–297. DOI: 10.1016/j.molcel.2009.04.025 [PubMed: 19450527]
54. Chen BP, Uematsu N, Kobayashi J, Lerenthal Y, Krempler A, Yajima H, Löbrich M, Shiloh Y, Chen DJ. Ataxia telangiectasia mutated (ATM) is essential for DNA-PKcs phosphorylations at the Thr-2609 cluster upon DNA double strand break. J Biol Chem. 2007; 282:6582–6587. DOI: 10.1074/jbc.M611605200 [PubMed: 17189255]

55. Finzel A, Grybowski A, Strasen J, Cristiano E, Loewer A. Hyperactivation of ATM upon DNA-PKcs inhibition modulates p53 dynamics and cell fate in response to DNA damage. Mol Biol Cell. 2016; 27:2360–2367. DOI: 10.1091/mbc.E16-01-0032 [PubMed: 27280387]

56. Reynolds P, Anderson JA, Harper JV, Hill MA, Botchway SW, Parker AW, O'Neill P. The dynamics of Ku70/80 and DNA-PKcs at DSBs induced by ionizing radiation is dependent on the complexity of damage. Nucleic Acids Res. 2012; 40:10821–10831. DOI: 10.1093/nar/gks879 [PubMed: 23012265]

57. Gamper AM, Rofougaran R, Watkins SC, Greenberger JS, Beumer JH, Bakkenist CJ. ATR kinase activation in G1 phase facilitates the repair of ionizing radiation-induced DNA damage. Nucleic Acids Res. 2013; 41:10334–10344. DOI: 10.1093/nar/gkt833 [PubMed: 24038466]

58. Schipler A, Iliakis G. DNA double-strand-break complexity levels and their possible contributions to the probability for error-prone processing and repair pathway choice. Nucleic Acids Res. 2013; 41:7589–605. DOI: 10.1093/nar/gkt556 [PubMed: 23804754]

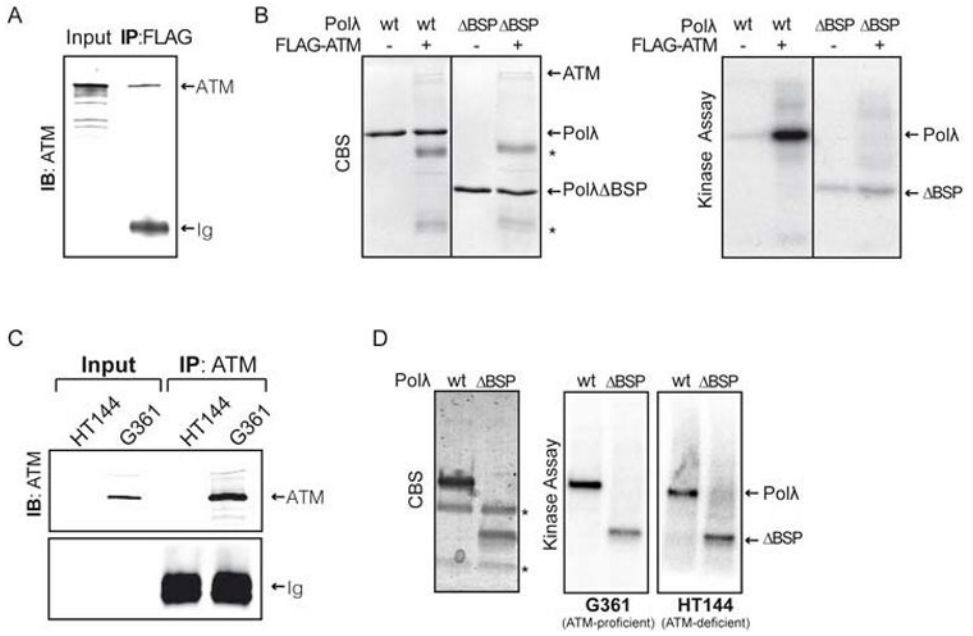

Figure 1. Phosphorylation of human Polλ by ATM-enriched immunoprecipitates *in vitro*.

(A) ATM was immunoprecipitated from 293T cells that were transfected with a FLAG-ATM encoding plasmid [29], and ATM was detected in the immunoprecipitates by Western blotting. (B) ATM-enriched immunoprecipitates were incubated with purified Polλ proteins in the presence of [γ-^{32}P]-ATP as indicated and samples were analyzed by SDS PAGE followed by Coomassie blue staining (CBS, *left)* and autoradiography *(right).* Polλ$^{\Delta BSP}$ indicates a Polλ deletion mutant lacking the two amino terminal domains (BRCT and S/P-rich). The position of purified Polλ proteins used in the assay is indicated on the right. Asterisks indicate the electrophoretic mobility of heavy and light immunoglobulin chains used in the immunoprecipitation of FLAG-ATM fusion protein. (C) Untagged ATM was immunoprecipitated from G361 (ATM-proficient) or HT144 (ATM-deficient) cell lines using monoclonal anti-ATM antibody (see Materials and Methods). (D) ATM-enriched immunoprecipitates were used in kinase assays as described in (B).

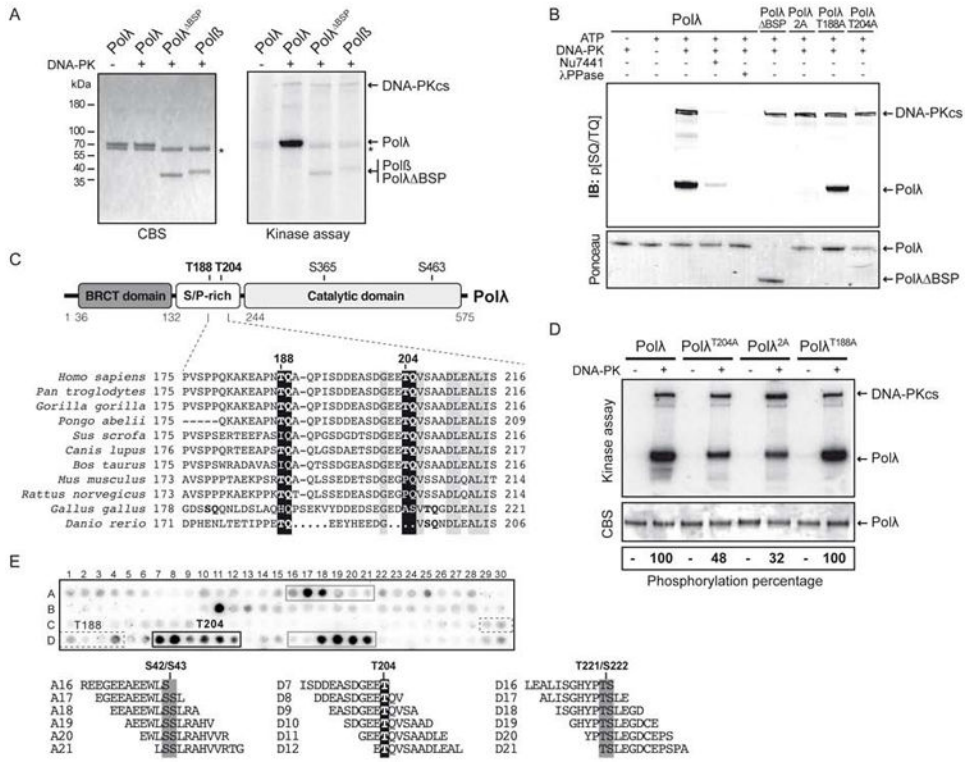

Figure 2. Human Polλ is phosphorylated by DNA-PKcs *in vitro* at T204

(A) Kinase assay using DNA-PK complex and purified recombinant Polλ proteins. Proteins were incubated with [γ-^{32}P]ATP with (+) or without (-) purified DNA-PK as indicated and samples were analyzed by SDS PAGE followed by Coomassie blue staining (CBS, *left)* and autoradiography *(right).* The position of the proteins used in the assay is indicated. Polλ$^{\Delta BSP}$ indicates a Polλ deletion mutant lacking the two amino terminal domains (BRCT and S/P-rich). Autophosphorylated DNA-PKcs on the autoradiogram is shown as an internal control in the kinase assay that represents equal kinase loading in all the samples tested. Polβ is shown as a control of Polλ phosphorylation specificity. Asterisks mark the position of bovine serum albumin. (B) Kinase assay and analysis of DNA-PKcs mediated Polλ phosphorylation by immunoblotting with anti-phosho[S/T]Q specific antibodies. The indicated purified Polλ proteins were incubated with DNA-PK, ATP, DNA-PKcs inhibitor NU7441 and A-phosphatase as indicated, and then analyzed by SDS-PAGE followed by Western blotting using a specific antibody for phosphorylated [S/T]Q sites. The position of phosphorylated Polλ and autophosphorylated DNA-PKcs are indicated. Ponceau staining of the purified proteins used in the assay is also shown *(lower panel).* (C) Schematic of human Polλ domain organization with main PIKK-dependent phosphorylation sites indicated. Boundaries of the different domains (BRCT, S/P-rich and catalytic) are indicated. PIKK-dependent phosphorylation sites located in the S/P-rich domain are marked in bold; *Bottom:* Sequence alignment of the 175–216 amino acid region of Polλ highlighting the conservation of PIKK consensus sites across species (white over black background). Threonine residues that are part of these sites are indicated, as are residues conserved in all species (grey boxes). (D) Single and double threonine (T) to alanine (A) Polλ phospho-blocking mutants were generated by mutations at T188 and T204 as indicated, and *in vitro* kinase assay with

purified DNA-PK was performed as described in A). Autoradiography shows phosphorylated Polλ and autophosphorylated DNA-PKcs in the kinase assay *(upper panel).* Coomassie blue staining (CBS) of the purified proteins used in the assay is also shown *(lower panel).* Band intensities were quantified using ImageJ and phosphorylation of mutants is indicated as the percentage of phosphorylation with respect to wild-type Polλ. (**E**) Kinase assay on peptide-scanning arrays covering N-terminal BRCT and S/P-rich domains using purified DNA-PKcs. Peptides containing conserved T204 are shown (marked with a black box) and their sequence is listed below the array. Other putative sites for DNA-PKcs targeting out of the [S/T]Q consensus motif are also indicated with grey boxes, and peptide sequences containing them are listed below the array.

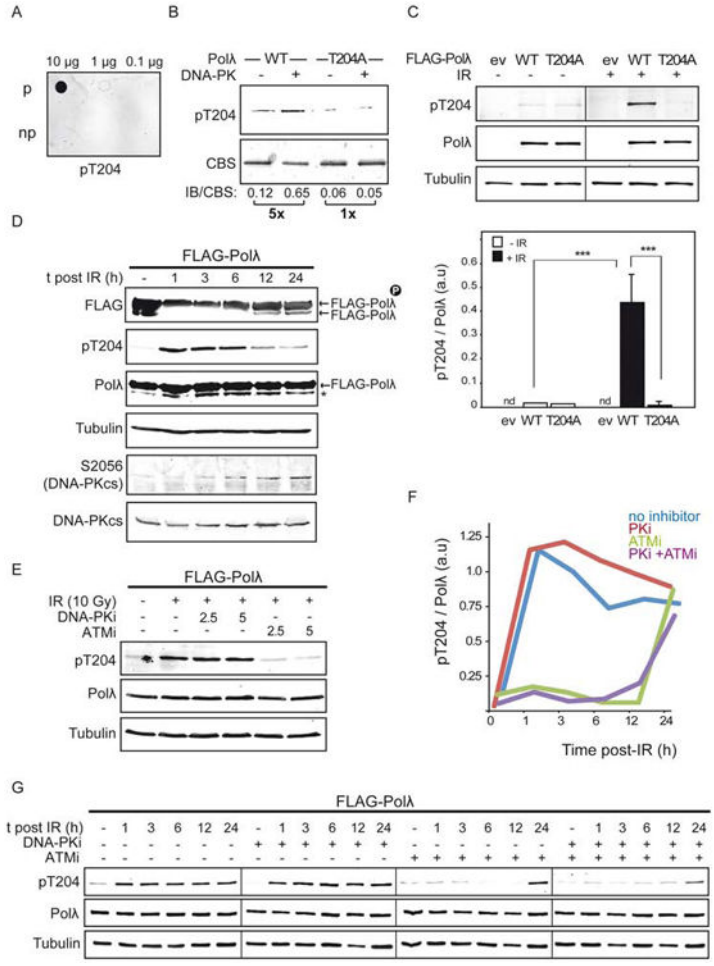

Figure 3. Human Polλ T204 is phosphorylated by ATM and DNA-PKcs *in vivo* in response to IR-induced DSBs

(A) T204 phospho-specific antibody (pT204) preferentially recognizes phospho-T204 (p) over non-phospho T204 (np) peptide. (B) Purified wild-type Polλ and phospho-blocking PolA-T204A proteins (250 ng) were assayed for DNA-PKcs kinase activity *in vitro* (Materials and Methods). T204 phosphorylation was detected with the pT204 phospho-specific antibody (IB). Total protein was visualized by Coomassie blue staining (CBS). Quantification of the corresponding bands was performed by using ImageJ. The ratio IB/CSB for each sample and the fold increase of T204 phosphorylation is indicated. (C) 293T cells transfected with FLAG-empty (ev), FLAG-POLL wild-type or FLAG-POLL T204Aplasmid were mock irradiated or irradiated with 10 Gy of IR and collected 1 h after irradiation. Cell extracts were obtained and proteins analyzed by SDS-PAGE and Western blotting for the indicated proteins. A representative experiment is shown. *(Bottom)* Quantification of T204 phosphorylation observed in two independent experiments. Band intensities were quantified using ImageJ and phosphorylated T204 (pT204) is represented as pT204/Total Polλ ratio. Statistical significance was determined with one-tailed Mann-Whitney test, *** $p<0.001$ (D) 293T cells transfected with a plasmid encoding wild-type FLAG-POLL were mock irradiated or irradiated with 10 Gy of IR and collected at the indicated time post-irradiation. Whole cell extracts were obtained and FLAG-Polλ

phosphorylation was analyzed by Western blot using anti-FLAG antibody. The same samples were also immunoblotted using Polλ-T204 phospho-specific antibody (pT204) as described in Materials and Methods, Polλ antibody (total Polλ control), tubulin antibody (loading control), phospho-Ser2056 DNA-PKcs antibody (control of IR-mediated DSB induction) and DNA-PKcs antibody (total DNA-PKcs control), as indicated. Asterisk indicates putative faster migrating untagged Polλ, representing either endogenous Polλ or some protein degradation, or a cross-reactive band. (E) Effects of ATM and/or DNA-PKcs inhibition on Polλ T204 phosphorylation. Human 293T cells were pre-treated with vehicle DMSO, the specific DNA-PKcs inhibitor NU7441 (2.5 or 5 μM) or the specific ATM inhibitor KU55933 (2.5 or 5 μM). One hour after addition of inhibitors, cells were left untreated or irradiated with 10 Gy of IR and collected 1 h after irradiation. Whole cell extracts were prepared and blotted for phosphorylated T204 (pT204), FLAG-Polλ (FLAG) and tubulin as described in Materials and Methods. The experiment was repeated twice with similar results. (F,G) Kinetics of T204 phosphorylation in human 293T cells treated with vehicle DMSO, the specific DNA-PKcs inhibitor NU7441 (5 μM), the specific ATM inhibitor KU55933 (5 μM) or both inhibitors together (5 μM each). One hour after addition of the inhibitor/s, cells were left untreated or irradiated with 10 Gy of IR and collected at indicated times after irradiation. Whole cell extracts were prepared and blotted for phosphorylated T204 (pT204), FLAG-Polλ (FLAG) and tubulin. Quantification of relative band intensities was carried out using ImageJ software. Levels of pT204 were normalized to total Polλ protein. Tubulin was used as a loading control. The experiment was repeated twice with similar results. A representative experiment is shown in (G).

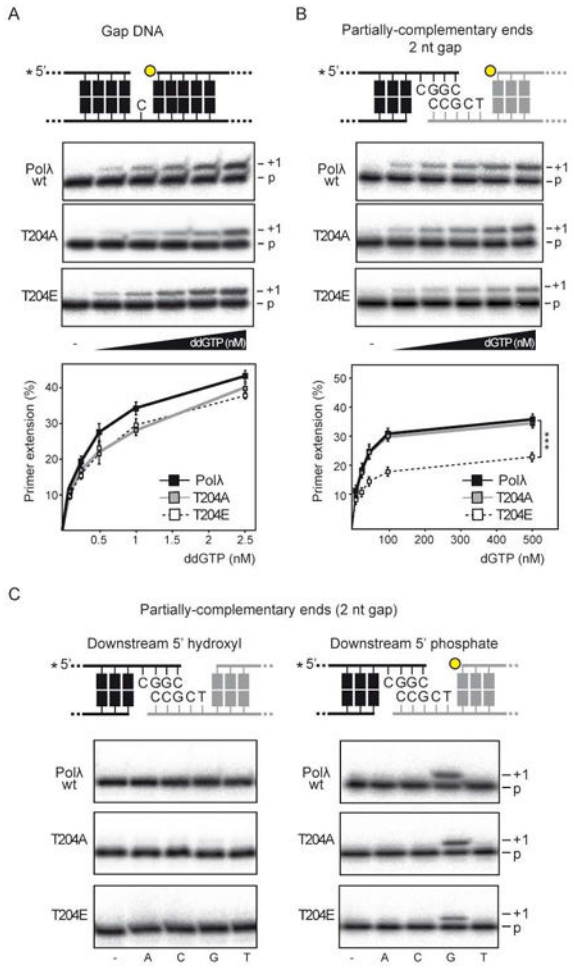

Figure 4. *in vitro* characterization of PolA-T204A and PolA-T204E phospho-mutant proteins

Polymerization assays were carried out as described in Materials and Methods. Specific 5′-[γ-^{32}P]-labelled gapped (A) and NHEJ (B) DNA substrates were incubated with 50 nM of either purified recombinant wild-type Polλ, Polλ-T204A phospho-blocking or Polλ-T204E phospho-mimic mutants in the presence of the indicated concentrations of ddGTP, to ensure that polymerization events were restricted to a +1 nt insertion. After 30 min at 30°C, primer extension was analyzed by 8M urea/PAGE and autoradiography. The positions of the labelled primer (p) and the +1 nt extension products are indicated. Statistical significance of the different kinetics of PolA-T204E mutant with respect to wild-type Polλ was determined with a non-linear regression fit using PRISM software, *** $p<0.001$. (C) Specific 5′-[γ-^{32}P]-labelled NHEJ DNA substrates, with or without a downstream 5′-phosphate group were incubated with 50 nM of either purified recombinant wild-type Polλ, Polλ-T204A or Polλ-T204E mutants in the presence of the indicated dNTPs and processed as in (A). The positions of the labelled primer (p) and the +1/+2 nt extension products are indicated.

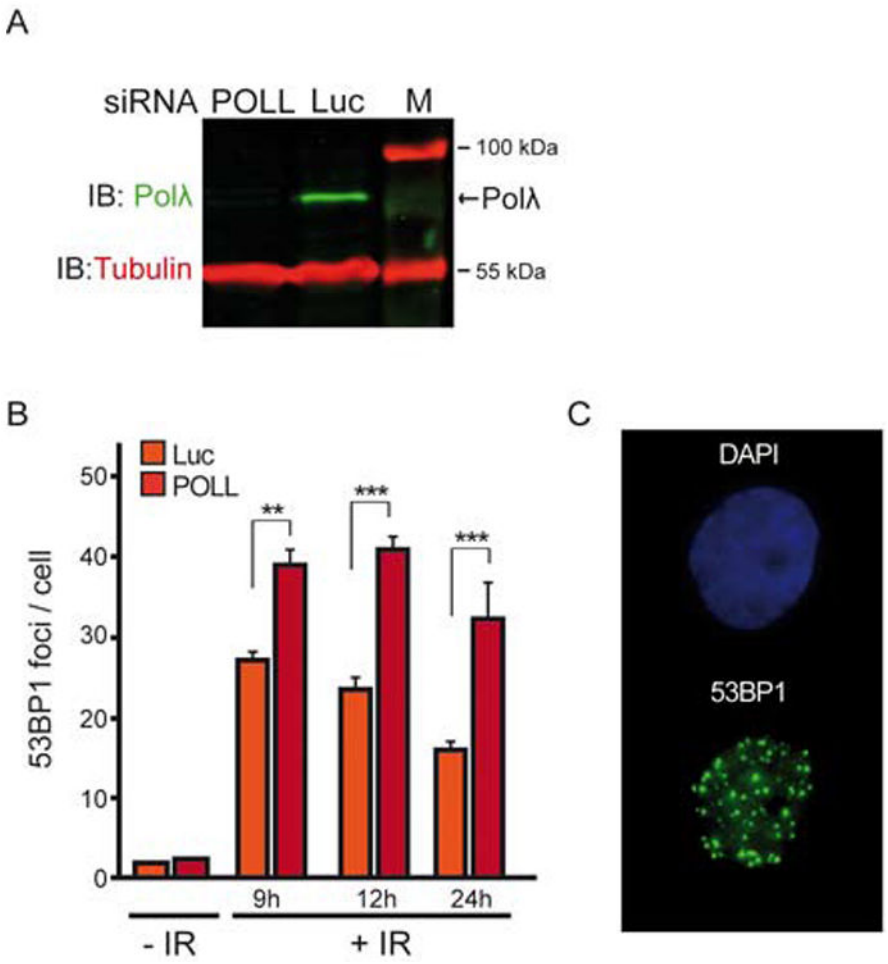

Figure 5. Polλ is required for an efficient repair of IR-induced DNA DSBs *in vivo*.

(A) *POLL* silencing in human U2OS cells. U2OS cells were doubly transfected with either siR-NA-*POLL* or control siRNA-luciferase (Luc) as described in Materials and Methods. Seventy-two hours later cells were collected and whole cells extracts obtained. Silencing efficiency was confirmed by Western blotting using anti-Polλ antibody. Electrophoretic mobility of human Polλ is indicated. (B) Dynamics of 53BP1 foci disappearance in cells silenced for *POLL* expression in response to IR-induced DSBs. U2OS cells were doubly transfected with either control luciferase siRNA or *POLL* siRNA. Seventy-two hours later, cells were irradiated with 10 Gy of IR, collected at the indicated times and co-stained for 53BP1 (green) and DAPI (blue). 53BP1 foci were scored for ≥ 50 cells per condition, via blind counting. Results represent the mean and standard error of the mean of three independent experiments. Statistical significance was determined by two-way ANOVA test with Bonferroni post-test correction, **p<0.01, ***p<0.001. (C) Representative image of the immunofluorescent identification of 53BP1 foci scored in (B) visualized in a fluorescence microscope. High-resolution z-stack images were obtained and then rendered into a 2D image showing DAPI stained nuclei (blue) and 53BP1 foci (green).

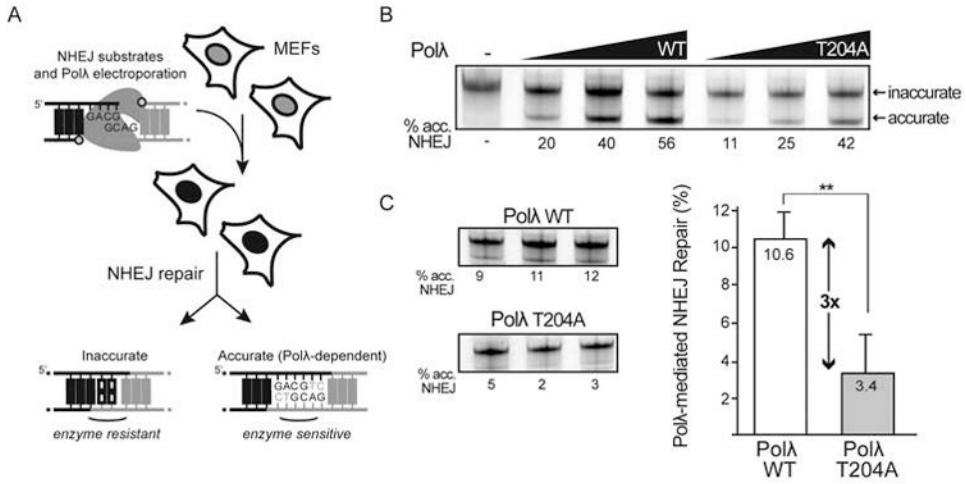

Figure 6. Extrachromosomal assay to specifically measure PolA-dependent NHEJ *in vivo.*

(A) Description of the extrachromosomal DSB repair assay. A linear DNA fragment with GACG3′ overhangs can align to generate a 2-nt gap with 5′-phosphate ends (described in cartoon). These DNA substrates were introduced into Polu-Polλ double-deficient mouse embryonic fibroblasts (MEFs) that were also complemented with either wild-type Polλ or T204A phospho-blocking mutant purified proteins. Repair products were recovered and amplified. Amplified products were subjected to restriction enzyme digestion using an enzyme *(AatII)* diagnostic for accurate (PolA-mediated) repair. (B) The GACG3′ NHEJ substrates were introduced into the polymerase-deficient MEFs together with increasing amounts (0.1, 0.2, and 0.5 ng) of purified Polλ or PolA-T204A proteins to identify the experimental conditions where Polλ was not saturating, and thus best-able to respond to phosphorylation-dependent regulation of activity. The percentage of junctions formed after PolA-mediated accurate synthesis is indicated. (C) The GACG3′ NHEJ substrates were introduced into the polymerase-deficient MEFs together with the lowest dose (0.1 ng) of purified proteins. The percentage of junctions formed after PolA-mediated fill-in of the 2 nt gap is indicated below the panels and the quantification of these experiments in shown in the plot. Results represent the mean and standard error of the mean of three independent experiments. Mean recovery efficiencies were assessed as significantly different using one-tailed Mann-Whitney test, **p<0.01.

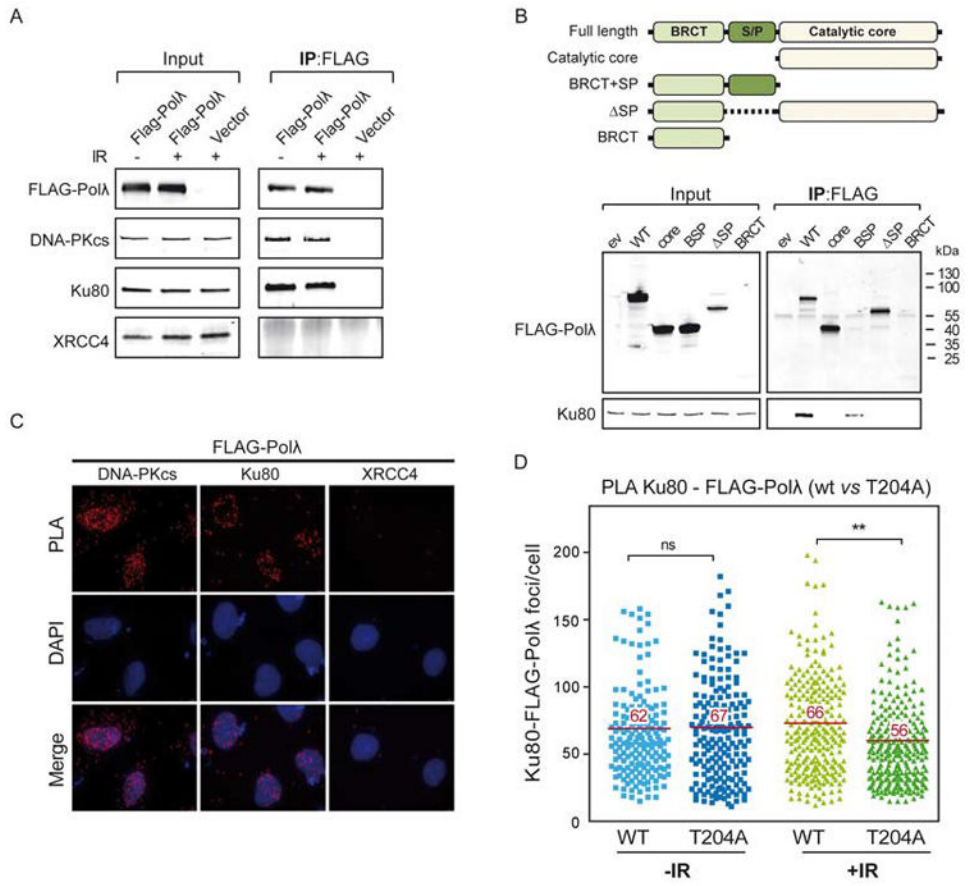

Figure 7. Polλ interacts with Ku80 and DNA-PKcs

(A) 293T cells transfected either with FLAG-empty or FLAG-POLL plasmids were mock irradiated or irradiated with 10 Gy of IR to induce nonspecific DSBs. One hour later, whole cell extracts were prepared and FLAG-Polλ was immunoprecipitated with anti-FLAG antibody (IP) in the presence of 20 U/mL benzonase and immunoblotted (IB) with the indicated antibodies. Input samples are 10% (v/v) with respect to IP samples. (B) 293T cells transfected with either FLAG-empty vector or plasmids encoding different FLAG-POLL deletion variants (a scheme is shown at top) were treated as in (A). FLAG-tagged proteins were immunoprecipitated (IP) in the presence of 20 U/mL benzonase, run in 4-20% gradient gels and immunoblotted (IB) as indicated. Input samples are 10% (v/v) with respect to IP samples. (C) Proximity ligation assays were performed to confirm *in situ* the interactions described in (A) and (B). U2OS cells overexpressing FLAG-Polλ were irradiated with 2 Gy of IR and examined 1 h after irradiation for PLA foci of FLAG (for PolA) and the indicated proteins by immunofluorescence. Nuclei were counterstained with DAPI and the PLA signals (red) were visualized in a fluorescence microscope (scale bars, 7.5 μm). (D) U2OS cells overexpressing either FLAG-Polλ or FLAG-Polλ-T204 were mock irradiated or irradiated with 2 Gy of IR, and examined 1h after irradiation for PLA foci of FLAG (for PolA) and Ku80 by immunofluorescence as described in (C). The plot shows quantification of PLA signal per nucleus from three independent experiments (at least 150 cells scored). Statistical analysis was performed first with Kolmogorov-Smirnov test, which indicates the non-parametric distribution of samples, and with Kruskal–Wallis One-Way test and Dunn's

post-test correction, ** $p < 0.01$ compared to wild-type Polλ transfected cells. Lines denote mean values.

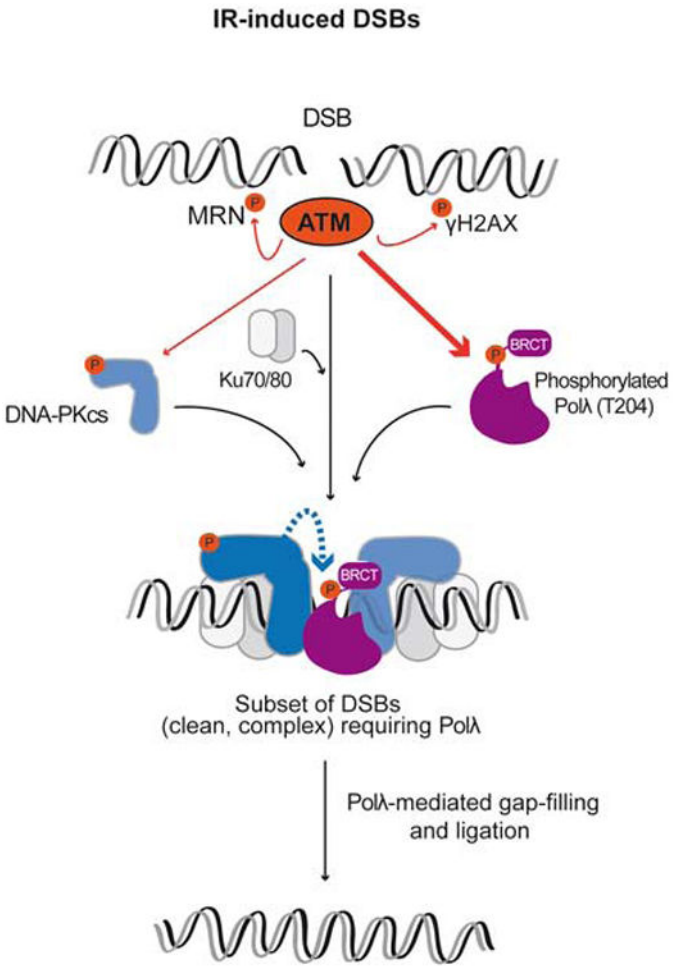

Figure 8. A model of IR-induced phosphorylation of Polλ T204 during NHEJ repair

Upon DSB induction with IR, different types of DSBs, representing different levels of complexity at their ends, must be repaired. A pivotal step in the DDR is the recruitment and activation of ATM by the Mre11-Rad50-Nbs1 (MRN) complex. Once activated, ATM phosphorates the MRN complex, histone H2AX and DNA-PKcs, among other targets. In addition, it phosphorylates Polλ at T204 residue, necessary for the repair of a subset of DSBs having either clean or complex DNA ends. T204 phosphorylation facilitates the formation of a stable complex of Polλ and DNA-bound DNA-PK, favoring an efficient Polλ-mediated gap-filling. Notably, in the absence of ATM, DNA-PKcs could also phosphorylate Polλ at T204, presumably with the same biological effect (indicated with a dotted blue arrow). Polλ is represented as a protein containing two globular domains joined by a linker representing the S/P-rich domain. Phosphorylation by ATM is indicated with orange arrows and circles.